

Mahua Biodiesel Blend with Nano Graphene Oxide Additive Emulsion on CRDI Diesel Engine Performance

¹P. Senthil*, ²B. Prem Anand, ³P. Rajkumar, ⁴C.G. Saravanan

^{1,2,3,4} Department of Mechanical Engineering, FEAT, Annamalai University,
Annamalai Nagar – 608 002, Tamilnadu

*consultsenthilau@gmail.com, prem.au2005@gmail.com, rajkumarme2014@gmail.com,
rsdk66@yahoo.com

Abstract

In order to increase the performance, combustion, symmetric features, and emissions of a customized common rail direct injection (CRDI) diesel engine, diesel, n-butanol, and GO nanoparticles are utilised. The study used a three-holed solenoid fuel injector and symmetric toroidal combustion chamber. This study examined how n-butanol and synthetic asymmetric graphene oxide nanoparticles affected Mahua biodiesel (MME20) performance. Nanofluids were made by dissolving different amounts nano-additive comprising asymmetric graphene oxide, sodium dodecyl benzene sulphonate (SDBS) emulsifier in n-butanol, and n-butanol as the solvent. MME20. Probe sonication prevented nanoparticles from aggregating in the base fluid for making nanofluids. Four stable and symmetric nanofuel mixtures were made from graphene oxide at 30, 60, 90, and 120 ppm. In this experiment, nanofluid, biodiesel, and n-butanol were used. Mahua biodiesel nanofuel mixes were subjected to a thermogravimetric evaluation and Fourier transform infrared spectroscopy for analysis. The nanofuel blend MME20B10GO90. Utilization and performance improved by growing the fuel injection pressure from 300 bar to 600 bar and then to 900 bar with pilot injection. Increasing the injection pressure improves the Results reveal BTE and combustion parameters. Graphene oxide nanoparticles' high catalytic activity and enhanced microexplosion phenomena improved the thermal efficiency of brakes (BTE) and reduced brakes-specific combustibility consumption (BSFC) under full load. All nano fuel blends outperformed Mahua sativa biodiesel in heat release rate heat release rate (HRR), smoke, hydrocarbons (HC), CO₂, and CO emissions. Note that NO_x emissions slightly increased. When mixed with 10% n-butanol and 90 ppm graphene oxide nanoparticles, Mahua biodiesel performs comparable diesel fuel.

Keywords: *Mahua methyl ester biodiesel, Graphene oxide Nanoparticles, Diesel engine CRDI, n butanol*

1. Introduction

Rudolf Diesel built his astonishing engine with vegetable oils a century ago. Diesel fuels and engines developed alongside inexpensive petroleum, In the 1930s and 1940s, during emergencies, vegetable oils were utilized as diesel fuels due to their ability to refine fuel-grade crude oil fractions. Since then, scientists have conducted extensive research on vegetable oils as a potential substitute for diesel fuel in highly efficient diesel engines. While the majority of research and development on alternative diesel fuels has been carried out in developed nations, the demand for such alternatives remains significant in developing countries. ability to produce them dramatically altered the industrial revolution. Diesalization's peak torque range and fuel conversion efficiency made it attractive in low-cost transportation and power applications. Diesel smoke harms the environment worldwide. In response to these issues, new stricter emission rules known as Euro 6 have been put in place to cut NO_x emissions by half and carbon monoxide emissions by more than 90 percent below Euro 5 standards. Improvements in engine efficiency, thermo-physical characteristics, heat transfer rate, fuel mixture equilibrium, and exhaust emission incorporation of nanoparticles, including metallic, non-metallic, oxygenated, organic, and amalgamated ones, into diesel-biodiesel emulsion fuels as a means to reduce emissions. The focus of this article is on the utilization of nanoparticle additives in diesel-biodiesel fuels. Exhaust after-treatment systems are expensive to install and maintain, so it may be worthwhile to look into alternatives, such as using oxygenated fuels, controlling smoke emissions in the cylinders with the help of additives, or combining with pilot, without pilot injection, and various injection pressure controls simultaneously for optimum performance. Engine-out smoke is caused by soot formation and oxidation, which burns off quickly as oxygen concentration rises.

Studied Since it's made from vegetable oils, biodiesel burns cleanly and doesn't pollute. Researchers detected 26 kinds of oil generated from methyl esters of fatty acids, which makes them appropriate for biodiesel [1]. Studied Diesel engines increase greenhouse gas emissions, urban pollution, and fossil fuel depletion. CO, NO_x, PM, and PAHs are released by diesel engines. [2,3] reported Euro 6 emission standards require automakers to lower exhaust-out NO_x by 50% and CO by 90% compared to Euro 5 [4,5]. reported Euro 6 requires light-duty diesel cars to reduce NO_x and CO emissions from 0.18 to 0.08 and 0.50 to 0.05 g/km, respectively [6,7]. observe Smoke opacity data is converted into soot concentrations via opacimeters. MIRA correlation calculates smoke data soot emissions index [8]. In their study, the researchers investigated the effects of pilot-pilot-main and pilot-main-after injection strategies on soot emissions, NO_x emissions, combustion noise, and brake specific fuel consumption. The details of this study can be found in reference [9]. Diesel engine emissions are reduced via pre- and post-combustion, biofuels, engine layout, and fuel additives. Light-duty diesel automobiles' particle filters and catalytic converters minimise emissions. High-pressure common rail, multiple, and multipoint fuel injectors, turbocharging, and supercharging air intake reduce pollution in diesel engines [10]. Biodiesel production is a promising field for study because of the environmental benefits and the increasing cost of GAeum. Emission-cutting fuels like biodiesel and diesel-biodiesel blends are currently the subject of research. [11,12]. To inject a pilot gas, use a split injection. In order to quiet the combustion process and make use of low cetane fuels, pilot injection was experimented with in 1937. The pressure buildup is limited and ignition is sped up by the

pilot injection. [13,14]. Premixed fires burn faster without an ignition delay. Researchers are looking into using pilot and split injection to cut down on NO_x from premixed combustion. [15,16] With no penalty to fuel economy, pilot injection and high-pressure injection can cut NO_x emissions by 35% and smoke emissions by 60-80% [17]. Shorter combustion periods around TDC improve efficiency, therefore it makes logical that trials using a 3 CA degree spacing for the injections revealed minor BSFC than those using an 8 CA degree arrangement. Studies show that split injection decreases NO_x emissions while slightly increasing particle emissions. Split-injection techniques cut down on emissions by continuing combustion far into the expansion stroke while reducing soot. Particle emissions might be reduced in comparison to the standard single-injection method by optimising injection characteristics to promote mixing [18]. Pilot and main diesel fuel injection, Erhard Sitter et al. A high-pressure injection pump drives a piston in a hydraulic pilot injection auxiliary pump, which then positively displaces a pilot injection amount. A storage piston in the main injection region is the first target of the high pressure injection pump's force. The fuel storage piston line is only present on the pilot injection piston stroke [19]. Diesel pollutant emissions may be reduced at a low cost with the use of fuel additives. Researchers are looking at nanomaterials as potential eco-friendly additions for diesel fuel. Liquid fuel is evenly dispersed by nanoparticles. Enhanced ratio of surface area to total volume [20,21]. Recent studies of diesel fuel additives have shown that adding nanoparticles made of energetic metals may improve both fuel efficiency and pollutants. Nanoparticles of Al₂O₃ and CeO₂ added to diesel or biodiesel improve engine efficiency and decrease pollution levels. Nanoparticles of Al₂O₃ in diesel fuel improve combustion speed [22]. Bio diesel with 20-80 ppm CeO₂ improved brake thermal efficiency and decreased PM, CO, and NO_x emissions. Nanoparticles of cerium oxide reduce emissions of hydrocarbons and nitrogen oxides [23]. Combustion byproducts from the metal oxide additions include airborne particles that may irritate the lungs and skin [24,25]. Chemical, physical, and combustion properties make graphite oxide a viable diesel-fuel addition. GO is carbon, oxygen, and hydrogen. GO nanostructures are oxygen-functionalized 2-D graphene sheet stacks. [26,27]. Graphite is oxidised via three techniques. Hummers used KMnO₄ and H₂ SO₄ to oxidise graphite, whereas Brodie and Staudenmaier used KClO₃ and HNO₃. GO [28] precursors are also produced by intercalating graphite with strong acids like H₂ SO₄, HNO₃, or HClO₄. [28]. Engine performance increased by 6%, bsfc by 20%, NO_x emission by 40%, CO by 60%, and UHC by 50% at 50 mg/L GNP. [29]. 50 mg/L GO improves engine performance most (p_{max} raised by 5%, bsfc dropped by 17%, NO_x emission reduced by 15%, CO by 60%, and UHC by 50%). [30]. High exothermic heat release from SWCNTs and GO in SDD and GDD fuels enhanced in-cylinder temperatures and heat release rates, resulting in higher NO_x levels than diesel. Diesel emits 9.2% less NO_x than GDD and SDD. Lean NO_x traps or selective catalytic reduction reduce high NO_x. B20G90 SFC drops 14.48% with GO [31]. In Ailanthus altissima biodiesels, the addition of nanoparticles has been shown to reduce CO emissions by 18% for B10G90 and UHCs by 27.47% for B20G90. However, when graphene oxide (GO) is included in biodiesel, it leads to a 12.54% increase in CO₂ emissions and a 7.93% increase in NO_x emissions [32]. Another study found that the addition of 50 mg/l multi-walled carbon nanotubes (MWCNTs) to a 40% n-butanol (JME40B) fuel resulted in significant reductions in CO, NO_x, and UHC emissions by 65%, 70%, and 50% respectively, compared to pure

D100 fuel [33]. It was observed that n-butanol increases NO_x emissions, even at a modest 10% blend and lower speeds. The NO_x emission rate was highest in the second WHSC mode (100% load and 55% speed) due to the SCR's lower operating temperatures at full load, with the worst emissions observed for n-butanol mix [34].

On the other hand, butanol was found to reduce exhaust gas temperature and nitrogen oxide emissions compared to diesel fuel, with NO_x emissions being 3.1%, 4.3%, 7.3%, 10.6%, and 13.5% lower than diesel at full load for Bu10, Bu20, Bu30, Bu40, and Bu50 blends respectively [35]. In an investigation of a DI-CI engine performance and emissions with 0-25% butanol, it was determined that a 20% butanol blend outperformed diesel fuel, resulting in lower emissions. Specifically, a compression ratio of 19.5, fuel injection pressure of 210 bar, and fuel injection time of 230 CA bTDC yielded reduced emissions and improved performance compared to diesel fuel operation [36]. When biodiesel-butanol blends of 5%, 10%, and 20% were used in a small diesel engine, it was found that these blends increased brake specific fuel consumption (BSFC), CO, and HC emissions while decreasing NO_x emissions and exhaust gas temperature. The addition of butanol increased CO emissions in biodiesel blends [37].

Additionally, the engine performance and emissions of biodiesel-diesel blends are influenced by the presence of n-butanol and diethyl ether. A 10% n-butanol addition surpassed a 5% blend, with reductions of 27% in smoke emissions, 8.8% in NO_x emissions, and 30.7% in CO emissions observed in biodiesel-diesel blends containing 10% n-butanol. Moreover, compared to a biodiesel (20%)-diesel blend, a ternary combination of 10% n-butanol-biodiesel-diesel exhibited a 3.9% lower BSFC [38]. Blends of biodiesel or vegetable oil diesel fuel were found to have higher combustion temperatures and lower expansion stroke temperatures, with diethyl ether having a greater effect in decreasing these temperatures during combustion and increasing them afterwards, while ethanol and n-butanol diesel fuel blends showed minimal impact on these temperatures. Regenerate response Diesel fuel mixtures reduce NO_x emissions with bio-fuel content. Diesel mixes with diethyl ether reduce pollution. Biodiesel emits CO. Vegetable oil or bio-diesel diesel fuel mixes reduce unburned HC emissions, but alcohol and diethyl ether blends increase [39]. Butanol reduced CO₂ and HC and increased BSFC, NO_x, and CO in vegetable oil-diesel (20:70). Some ternary combinations may impact engine performance [40,41,42]. Graphene oxide nanoparticles in dairy scum oil biodiesel increased brake thermal efficiency (11.56% for DSOME2040) and reduced fuel consumption (8.34%). Nano fuel blends' NO_x emissions increased with viscosity, oxygen, flame temperature, and cetane number. NO_x decrease: 5.62% Best was DSOME(B20). Any biodiesel source increased NO_x [43]. Graphene oxide (GO) nanoparticles in diesel/biodiesel blends reduced VOC, CO, and BSFC emissions but increased NO_x emissions. Power increased using camelina biodiesel. [44]. found that combining GO nano-particles with biodiesel decreased CO and UHC emissions while increased CO₂ and NO_x emissions in fuel mixes. At full load, the B20GO90 blend produces the least CO. Adding GO nanoparticles to biodiesel may increase engine performance and cut emissions. Emissions decrease with GO nanoparticles. [45] GO possesses oxygen-reactive areas and high surface-to-volume ratios. Functionalized graphene sheets (reduced GO) increased liquid monopropellant nitromethane's linear burn-rate and ignition temperature. 29

Inspired by these findings, we perform a single droplet experiment to examine diesel fuel dosed with GO's combustion properties to determine its environmental friendliness. [46].

The most efficient diesel blends employed 75% transesterified mahua oil. Transesterified mahua oil enhances thermal efficiency at 25% diesel mixes. [47]. All 10%–30% mixes produce less NO_x than diesel. Pure alcohols burn without soot since they don't include inorganic components like sulphur. Particulates should not be released by alcohol-fueled diesel engines. Methyl esters, which include alcohol, release less particles than diesel. Diesels released more PM than 10%, 20%, and 30% mixes. Diesel engines may utilise 30% MOME mixed with 70% plain diesel. [48] A catalyst converts triglyceride and alcohol into glycerol and ester. Ester molecules, one-third the size of oil molecules, are low-viscous. 3:1 alcohol-to-triglyceride is needed for stoichiometric transesterification. A greater alcohol-to-oil ratio is used for low-viscosity, high-conversion biodiesel. [49,50]

Compression ignition engine fuels derived from vegetable oils increased production and consumption. It will include historical background, present and anticipated crop yields, vegetable oil conversion to diesel fuel technology and economics, oil performance, diesel fuel coproduction, environmental considerations, and future research. Diesel won't be replaced by vegetable oils. [51]. At 0.1% and 0.01% dosing doses, graphite oxide (GO) nanoparticles with aluminium oxide (Al₂O₃) and cerium oxide (CeO₂) nanoparticles enhanced diesel fuel combustion and decreased diesel engine pollutant emissions (PM, NO_x, PAHs, and CO). Thus, GO may be a diesel fuel additive that reduces pollutants and fossil fuel depletion. [52]. Nigella sativa's CO₂, HC, smoke, and CO emissions decreased by GO NPs. NSME25B10GO90's smoke, HC, and CO emissions at maximum load were 31.68%, 48.571%, and 50.15% lower than NSME25. [53].

Dodecylbenzene sulfonic acid, 28-65% 6-8% alkali, 0-8% cosolvent, 0-1% additive, and water make up sodium dodecyl benzene sulfonate aqueous solution. Aqueous sodium dodecyl benzene sulfonate is produced by the invention [54]. SME20 graphene dispersions were compared to two standard surfactants at optimum concentration by absorbance. Graphene was detected using nanofluid UV–Vis. Nanofluid absorbance decreased with static time for any surfactant concentration utilising UV–Vis spectral technique. In simarouba biodiesel-diesel blends, a 1:4

graphene-surfactant ratio maintains dispersion. In Simarouba biodiesel blends with diesel, SDBS disperses graphene better than SDS[55]. Colloidal suspensions, modest concentrations of colloids spread throughout a liquid hydrocarbon fuel, have been used to promote ignition and optimise fuel performance[56,57]

2. Research objectives and motivation

GNP with n-butanol as diesel additives improved CO, HC, and NO_x combustion and emissions in previous research. In previous studies, fluctuations in the smoke content of the fuel-additive blend were not taken into account because the ratio of NO_x to smoke is an issue that arises with compression ignition engines. In this study, GO and GNP are compared against diesel and biodiesel mixtures, as well as other fuels, in order to investigate combustion, smoke emissions, friction, and filtration. GNP additives for the combustion and emissions of diesel and mahua methyl ester biodiesel with varying fuel injection pressure.

3. Madhuca indica)

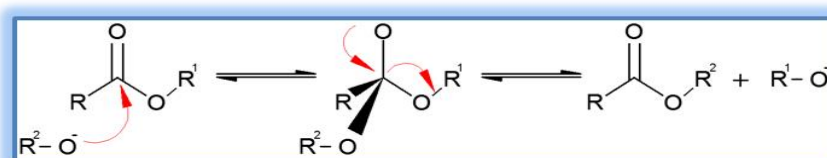
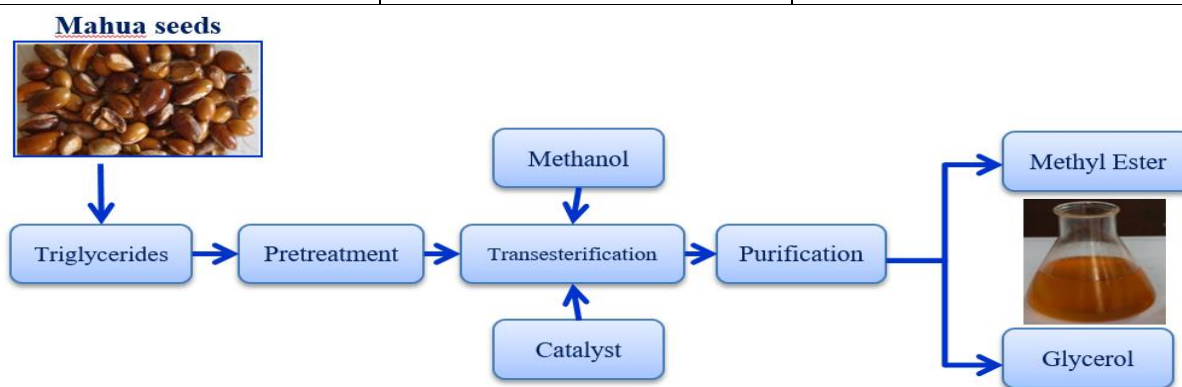
Mahua-derived oil. Forty recent study on Mahua Biodiesel's synthesis, application, and efficacy were examined. The characteristics of biodiesel, its blends, diesel, and the methods used to create blends, performance, and exhaust emissions have been compiled into a review paper. Blends with a catalyst burn and emit more efficiently than diesel alone. As a result, the researchers have a better understanding of mahua oil extraction, its use (blending with different proportions), bio-diesel catalysts, and the best blend for emission efficiency.

4. Biodiesel production

The family Sapotaceae includes mahuas. Northern climates support the expansion of Indian tropical plants [14]. It may reach a height of 20 metres in no time. Mahua oil has the potential to displace other fuels due to its abundance. The domestic and regional agricultural economy will benefit from mahua oil's commercialization as a replacement fuel. The fatty acid profiles of biodiesel made from mahua oil are shown in Table 1.

The fatty acid profiles of mahua oil biodiesel are shown in Table 1.

Fatty acids	The percentage of mahua oil by weight	The proportion of total biodiesel that is made from Mahua.
Palmitic	23.59	23.52
Stearic C18:0	18.77	18.91
Oleic C18:1	38.69	39.1
Linoleic	19.77	18.01
Linoleic	1.48	1.58



Source: Shafi T et al., 2015
Mechanism of transesterification process

Fig. 1 Transesterification process

There are several tried and true methods used in biodiesel manufacturing. Veggie oils can be converted into diesel fuel with little tweaking. Alcohol and a catalyst, such as potassium or sodium hydroxide, are used to trans esterify the molecules of raw vegetable oil into ethyl or methyl esters and glycerin. Using potassium hydroxide as a catalyst, biodiesel reactors whirl 7 grammes into 1 litre of methanol. Mahua oil is mixed with the catalyst/methanol.

After one hour of constant stirring at 60 °C and atmospheric pressure, the mixture is complete. The byproducts of transesterification include methyl ester and crude glycerine. Oil from Mahua, Table 1 Unrefined glycerin sinks after settling. After settling for a few hours, the phases will separate. Methyl ester needs 8-10 hours to settle.

An MME that has been washed twice. Combine 1 gramme of tannic acid per liter of water with 26% vegetable oil to make a wash solution for the methyl ester. Do away with the methyl ester. The transesterification process gave both methyl esters a diesel-like aroma and flavour. Blends of biodiesel (B20) were produced by adding MME to straight fuel. displays a flowchart of catalytic transesterification and the construction of a biodiesel plant.

5. Experimental setup

The Kirloskar AV1, a diesel engine with a single cylinder, four valves per revolution, water cooling, and common rail direct injection. The engine produced 3.7 horsepower. The engine turned at 1500 rpm while injector pressures varied between 300 bar and 900 bar. In order to maintain a steady engine speed for the pressure, the fuel injection lasted 650-1200 microseconds. Table 2 lists the engine's specifications, while Table 3 details information on the vehicle's fuel injectors. Figure 2 depicts the experimental setup schematic, and Figure 3 shows a common-rail schematic design.

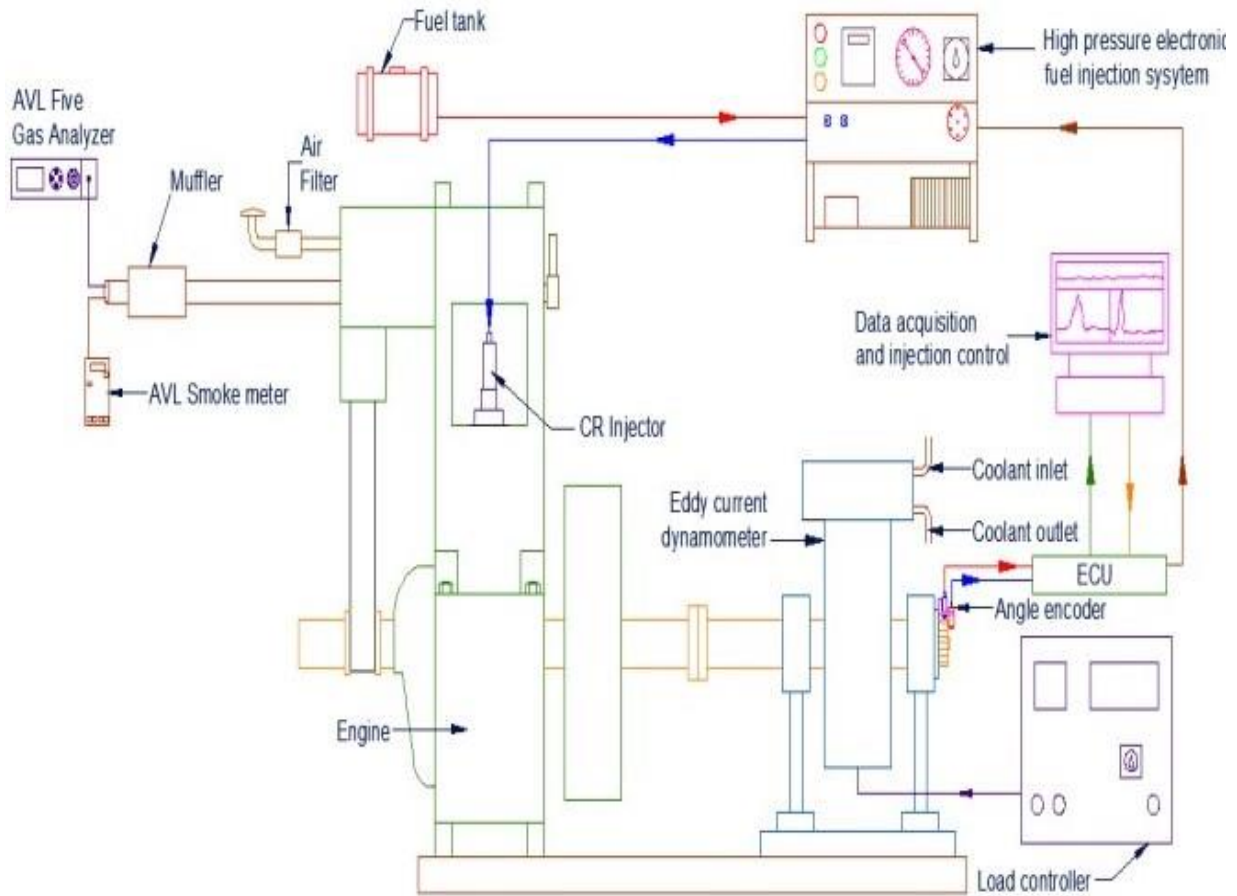


Fig. 2. CRDI Experimental setup

Type	CRDI engine with a single cylinder, vertical orientation, water cooling, and four strokes.
Brand	Kirloskar Engine
Power	3.7 kW
Stroke	110 mm
Bore	80 mm
Speed	1500 rpm
Compression ratio	17.5:1
Injection pressure	Variable from 300 bar, 600bar, 900bar
Mode of starting	Manually cranking
Orifice diameter (Air mass flow measurement)	20 mm

Table 2 Engine specifications

A single injector and a mass-produced Kirloskar high-pressure pump prototyped the high-pressure side. Engine running at 1500-rpm. The injection-pressure range was maximised by running the high-pressure zones fuel pump in a way that was not reliant on the functioning of the rest of the engine. maximum level.

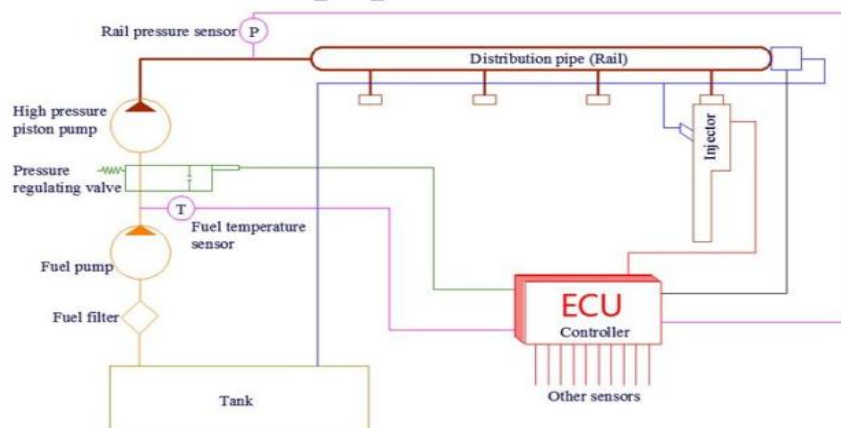


Figure 3 depicts a common-rail schematic design.

Fuel fed	Units	Common rail
Injection pressure	MPa	20-100
The total number of holes in the nozzle	-	3
Diameter of the nozzle hole	Mm	0.518
Initial Injection Start	-	23° Before top dead centre (BTDC)
Amount of time needed for an injection	µsec	650-3000

Table 3 Fuel injector system specification

The injection pressure is regulated by pressurizing just the required quantity of diesel via a production input metering valve. High-frequency signals would operate the injector spill valves to regulate pressure. Fuel pressure was managed via a high-pressure valve installed on the rail since neither a 16-bit controller nor enough spill flow was readily available. A filtering process lies at the heart of AVL 415's functionality. Reflecting photometers calculate Hatridge Smoke Units (HSUs) from filter paper darkness. The investigation employed AVL Digas gas analyzer. Linearity measures of +/-1% and accuracy readings of 2% were taken over the course of 8 hours using the system.

6. Graphene oxide (GO)

Graphene is hexagonal carbon atoms. Two-dimensional graphene. Graphene conducts electricity and heat best. Graphene can be utilised in electronics, medicines, biodiesel fuel additives, aeroplanes, and more.

Researchers have been looking for cheaper alternatives to graphene with equal advantages because of its high cost and complicated production. Graphite, which is both inexpensive and plentiful, is oxidatively broken down into (GO), a 1-atomic-layer molecule. Graphene oxide is graphene with oxygen added to it. Graphene, which may be formed when the material is spread in water (or other solvents), is simple to manipulate. It is possible to increase graphene oxide's conductivity. Common forms include a powder, a liquid, a biodiesel fuel additive of variable parts per million, or a coating.

7. Nanoparticle Stability Mechanisms

The stability of distributed nanofluids is threatened by particle aggregation. When the ultrasonic energy is no longer present, the nanoparticles will reunite due to Van der Waals forces. Recombination may be blocked by a variety of factors, including repulsion (steric, electrostatic, or electrosteric) or a similar refractive index. Particles aggregate when their mutual attraction is stronger than their mutual repulsion. Particle agglomeration is avoided and stability is maintained when repulsion is greater than attraction. High-shear mixing using a magnetic stirrer and ultrasonication were employed in this research. In order to prevent agglomeration in the continuous phase solvent, mechanical dispersion and chemical surface functionalization using surfactants (surface active agents) are used [58]. Surfactants provide stability via electrostatic and steric interactions. Repulsion prevents surfactant-coated nanoparticles from re-aggregating [59].

Deterrent, moistening, foaming, emulsifying, and dispersing, SDBS is a high-anionic surfactant. Parameters for improving graphene oxide dispersion with SDS and SDBS surfactants. A certain ratio of surfactant to graphene oxide is necessary for optimum dispersion.

8. Concoction of Fuel Blend

In this research, a probe sonicator is used to indirectly sonicate a mixture of SDBS surfactant and distilled water containing graphene oxide nanoparticles. The oxygen concentration of biodiesel may be increased by ultrasonication and NPs with 10% n-butanol. A magnetic stirring device, ultrasonicator bath, and probe sonicator add graphene oxide nanoparticles to fuel mixtures at 30, 60, 90, and 120 mg/L. MME20B10GO30 fuel mix contains 30 ppm graphene oxide NPs and 15 ppm SDBS surfactant. 25 ppm SDBS surfactant with MEME20, 10 mM B10GO60, and 60 ppm GO NPs. MME20 biodiesel is combined with 90 or 120 ppm graphene oxide nanoparticles and 35 or 45 ppm SDBS surfactant to make MME20B10GO90 and MME20B10GO120 fuel. In order to create nanofluids, you will need 5 millilitres of distilled water, graphene nanoparticles, and SDBS surfactant. These components will then be subjected to ultrasonic waves at a frequency of 20 kilohertz for 20 to 30 minutes.

Sonication prevents particle aggregates by breaking the symmetry of particles and disrupting intermolecular connections. Then, the MME20 biodiesel is combined with the nanofluids, swirled with a magnetic agitator at 60 degrees Celsius for 15 minutes to eliminate H₂O and moisture, blended in a bath-type sonicator for an hour each, and then sonicated in a probe sonicator to increase nanoparticle stability. Using these methods, stable nanofuel mixes may be created. Characteristics of fuel mixtures' physiochemistry

Properties	Unit	ASTM Standard (D6751-15C)	Diesel	MME20	MME20B10GO90
Kinematic Viscosity	cSt @ 40 °C	ASTMD445	2.35	4.789	3.312
Calorific	MJ/kg	ASTM D5865	45.458	40.98	42.89

Value					
Density	Kg/m ³ @ 15 °C	ASTM D4052	822.89	864.89	849.95
Specific Gravity	gm/cc	ASTM D891	0.8	0.858	0.852
Flash point	°C	ASTMD93	78	132.59	108.54
Four Point	°C	ASTM D97-12	-4	3.1	2.01
Cloud Point	°C	ASTM D2500-11	-1	5	5.41
Cetane Number	-	ASTMD 613	49.52	44.56	51.12

Table 4 Physiochemical traits associated with diesel, Mahua methyl ester, and nanofuel blends

9. Result and discussions

9.1 Features of CRDI Engine Combustion

9.1.1 The Influence that Fuel Additives on the Cylinder Pressure (CP)

The optimum cylinder pressure in a diesel engine is determined by the amount of fuel consumed during the pre-mixed stage of combustion. The angle between the compression stroke and the horsepower stroke affects CP. When the engine of an automobile is operating with uncontrolled combustion, the

quantity of MME20B10GO90 Nanofuel that is consumed is directly connected to the pressure that exists inside the cylinders of the engine. The fluctuation in the cylinder's pressure during full load is shown as an expression of crank angle in Figure 4, which may be seen below.

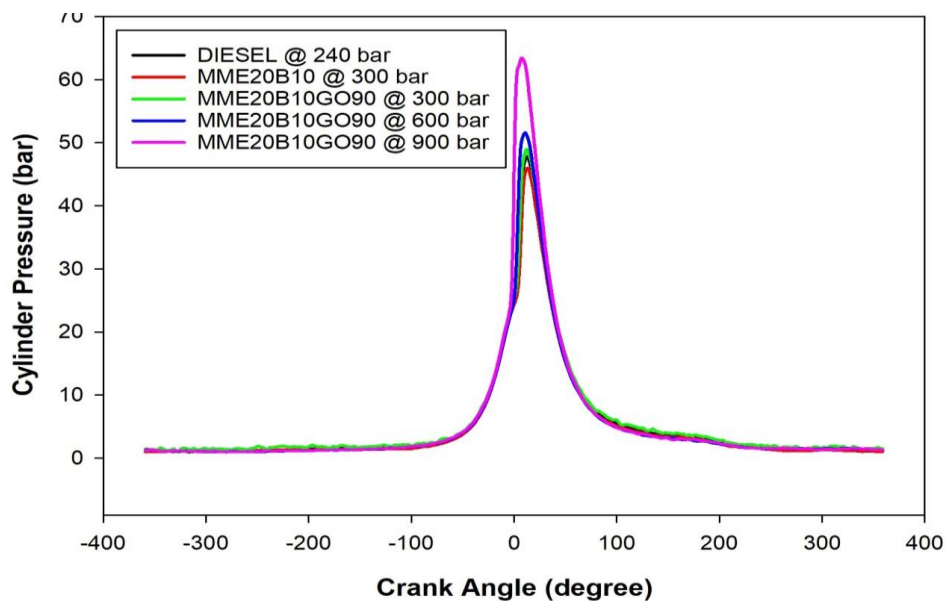


Fig.4 Full-load cylinder pressure and crank angle variations for all test fuels.

Following the incorporation of 90 milli grammes per litre of the GO Nanoparticles and 10% n-butanol into the solution, a significant volume-to-asymmetric surface-area ratio was observed. was achieved, which resulted in an increase in oxygen generation and an improvement in cetane content. When contrasted with the other nanofuel blends, it was discovered that each one performed much better than the others.

9.1.2 The Fuel Additives' Heat Release Rate

The fuel vaporisation and cylinder wall heat loss during the Combustion Delay phase lower the HRR. There are two aspects that may be ascribed to the enhanced HRR that has been found with nanofuel mixes across the board. These aspects include a quicker identification time as well as a stronger cetane number. When taken together, these two characteristics contribute to an increase in the overall effectiveness of the engine [42–45]. Figure 5 is an illustration of the HRR values and crank angle discrepancies that take place under situations of full load.

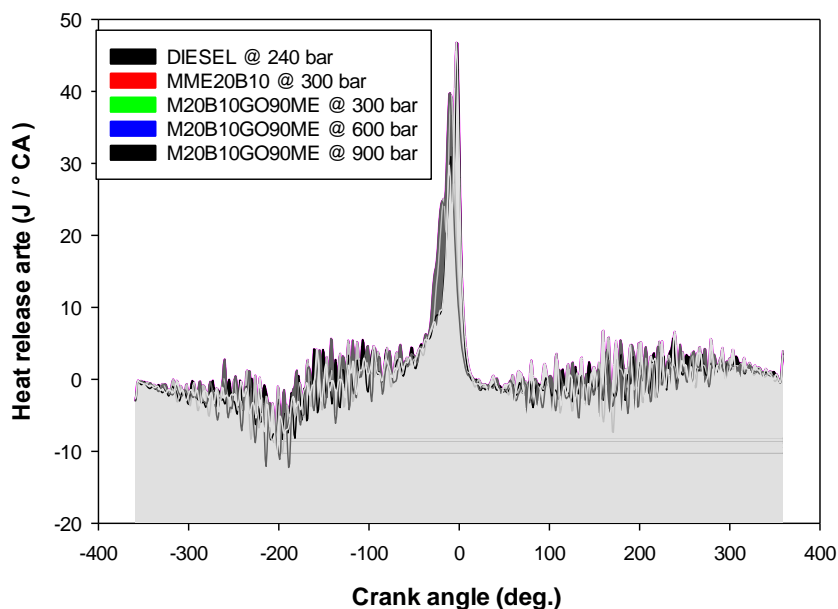


Fig.5 Test fuels' effects on HRR and crank angle at maximum load.

The greater molecular weight of the MME20 combination as well as its slower burning velocity are two variables that contribute to its lower HRR [46]. The overall HRR is increased when using nanofuel blends because to their increased surface area to volume ratio, rapid ignition, and improved fuel properties and thermal conductivity. Because of this, the peak pressures are far higher than normal. and the HRR both rise. MME20B10 GO reached its highest point of 90.54 J/CA, while diesel reached its highest point of 91.997 J/CA and MME20 reached its highest point of 60.813 J/CA. After adding A disparity of 29.727 J/CA was found between the HRR of a mixture containing pure MME20 and one comprising 90 Parts per million GO and 10% volume n-butanol.

9.1.3 Implications of Ignition Delay (ID) Period Modifiers in Fuel Blends

The Pre-combustion processes in the fuel-air mixture create the chemical delay, while the vaporisation, atomization, and blending of the fuel-air combination generate the physical delay, both of which contribute to the ID in the combustion chamber [48]. The chemical delay is what causes the pre-combustion processes in The physical delay vaporises the fuel-air mixture. The chemical delay arises because fuel-air pre-combustion processes must end before the reaction can begin. Figure 6 shows braking power increasing as ignition delay duration decreases. This pattern can be observed in the graph.

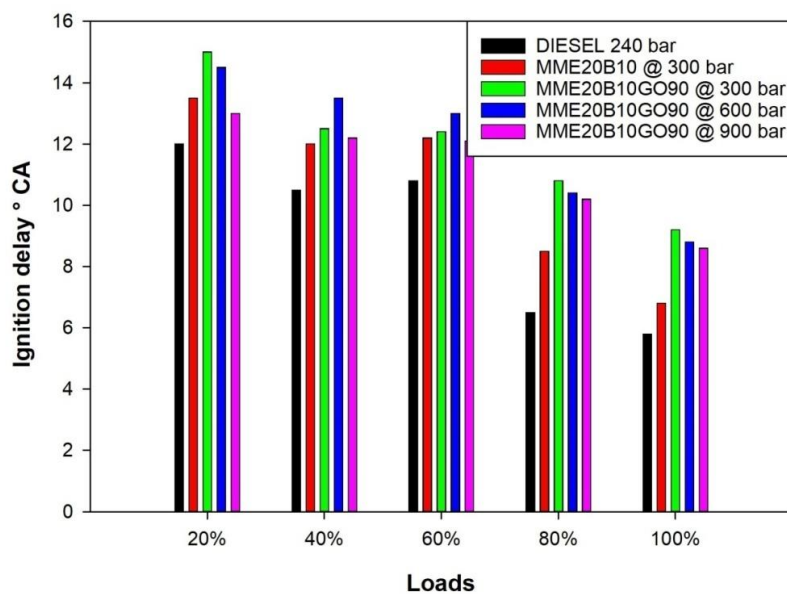


Fig.6. Test fuels with varying maximum loads and ignition delay times, and braking power variations.

The most adverse fuel quality is caused by Mahua biodiesel (MME20), which results in the longest delay. The biodiesel with 90 Parts per million GO NPs and Ten % n-butanol had values that were more comparable to diesel as a result of its superior combustion. The ID of MME20 (10.2 °CA) was much longer than that of MME20B10GO90 (8.11 °CA), which may be because MME20 has a greater viscosity. The ignition delay causes an increase in engine temperature, which accelerates and symmetrically burns all mixes, resulting in a reduction in the amount of braking power available. [15]. Mixing of air and fuel results in improved combustion via secondary atomization and microexplosion, which results in a decrease in ID. When loaded, diesel fuel has an ID that is 4.45 CA lower than when it is unloaded. Regardless of the load, Diesel and MME20B10GO90 fuel mixtures displayed ID times that were identical.

10.1 Fuel additive' impact on brake thermal efficiency (BTE)

Brake thermal efficiency, often known as BTE, is a metric that measures the stresses placed on an engine by converting fuel thermal energy into mechanical power. At constant load, graphene oxide NP dosages are administered to the boosted CRDI diesel engine BTE. Figure 7. Carbon-based nanoparticle oxides improve fuel charge the combustion process, unlike

diesel—biodiesel fuel mixes. Graphene oxide has oxygen-buffering capabilities, which contribute to BTE's enhancement. Graphene NPs have been shown to enhance BTE. When compared to clean MME20B10, the BTE performance of Mahua biodiesel containing 90 Parts per million GO NPs and 10% n-butanol was improved by 18.37% at maximum load [30]. The BTE declines considerably at 120 ppm of asymmetric GO NPs, which results in an intensification in the viscosity and density of the fuel mix. MME20B10GO90 nanofuel blends showed BTE values close to diesel. Increases in BTE can be observed for all nanofuel pairings under particular loads owing to the increased catalytic activity found in MME20B10, GO NPs, and the subsequent rise in the occurrences of symmetric micro-explosions that results from this activity.

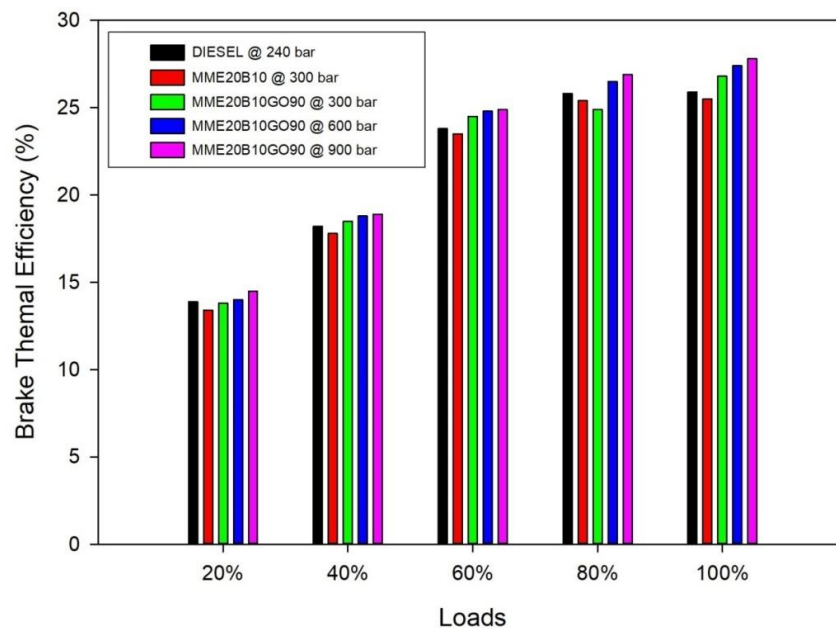


Fig.7. Brake Thermal Efficiency Vs Loads.

10.2 The Impact of Additives on BSFC (Brake-Specific Fuel Consumption)

The ability of CRDI diesel engine to create shaft power while also totally combusting the fuel charge is referred to as BSFC. This is the proportion of fuel used that corresponds to the amount of electricity produced. The length of the delay in ignition is mostly determined by the cetane rating of the fuel mix, which is a influence that plays a significant protagonist in the delay. As a result, the cetane number is an essential characteristic of diesel fuel that has a significant bearing on the CD. The atomization of fuel has a counterintuitive relationship with both the viscosity of kinematics and density of [52].

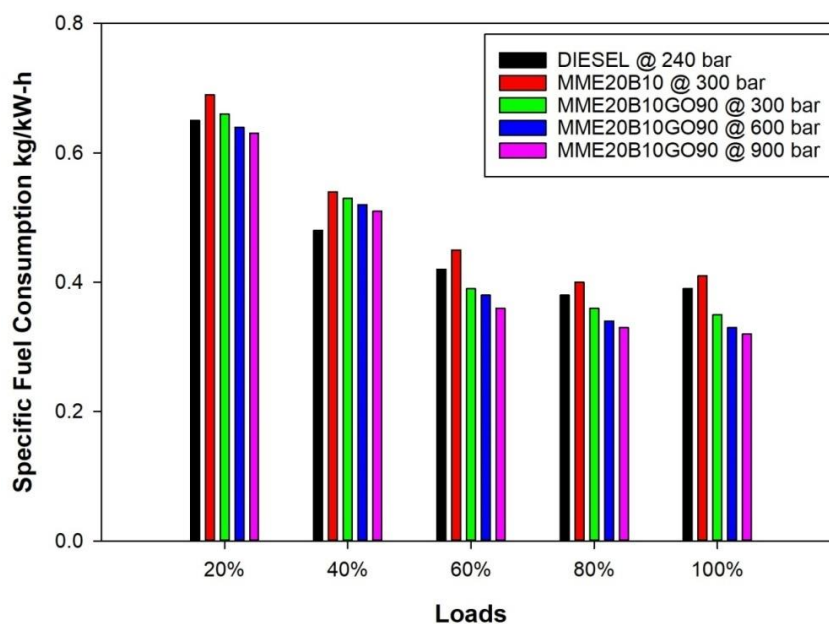


Fig. 8. BSFC vs Injection Pressure.

The BSFC full load aimed at various fuel blends are shown in Figure 8, which demonstrates the varying BP. Because of the excessive viscosity and density of MME20 blends, fuel atomization is hampered by these characteristics. However, the accrual of n-butanol condenses viscosity, in turn boosts the calorie content and cetane number by enabling more complete combustion. Microexplosions are amplified by GO NPs because of the high enzyme capacity and sensitive surface area that they possess [25]. The Mahua biodiesel has additives that improve combustion and minimise fuel usage. At full load, the MME20B10 GO 90 ppm GO had BSFCs of 312, 345, and 258 grammes per kilowatt-hour, respectively.

11. Traits of Emissions Produced by Engines

11.1 The Impact of Fuel Additives and Emissions of Carbon Monoxide (CO)

Emissions of carbon monoxide are caused by the incomplete and asymmetrical oxidation of fuel that occurs in the combustion chamber. In

order to achieve instant acceleration and start the engine, a strong A:F combination is required, which results in the production of CO. Because hydrocarbons do not contain any oxygen molecules, they are able to transform atmospheric carbon dioxide into CO. Figure 9 shows the test's CO and BP range.

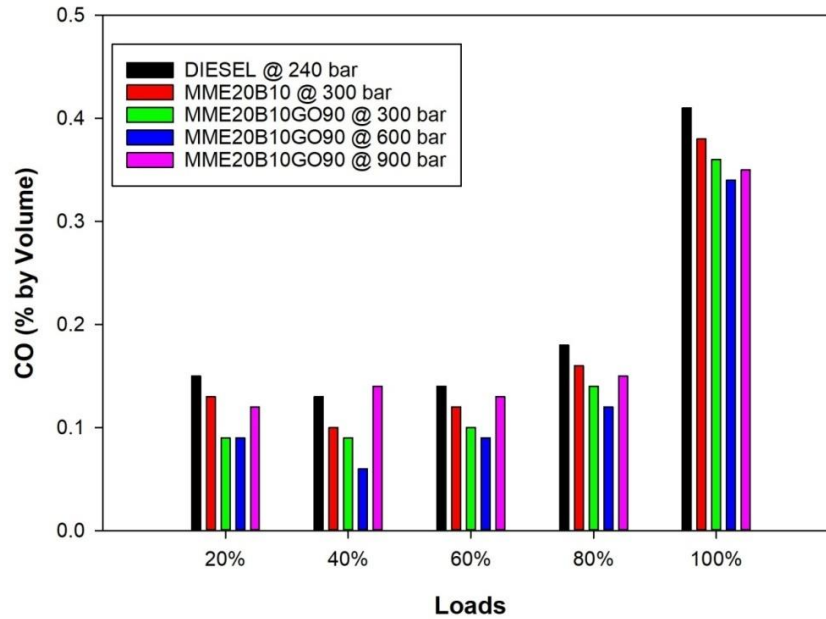


Fig 9: Emission of Carbon Monoxide.

Efficient fuel combustion and reduced CO emissions were made possible by diesel fuel's low density, high calorie content, and high rate of heat release [23,59]. Because of its high density, high viscosity, and poor combustion rate across the board, MME20 released an excessive amount of CO into the atmosphere. This was caused by its rich A:F combination, insufficient oxygen in the combustion chamber, excessive density, and high viscosity. Rapid combustion may be achieved by combining asymmetric graphene nanoparticles made of oxide with oxygenated additives like butanol [57]. MME20's graphene oxide and butanol boost the fuel's ability to oxidise, burn quickly, produce heat, and lower the combustion chamber's temperature. When compared to MME20, MME20B10+GO 90 ppm resulted in a 54.15 percent decrease in CO emissions. At 90 ppm GO, the CO emissions from MME20 were on par with diesel fuel. As a result, CO emissions may be converted to safe CO₂ using GO NPs and n-butanol.

11.2 The impact of Fuel Additives on Hydrocarbon (HC) Emissions

Graphene oxide nanoparticles included in the fuels induce the carbon atoms in the combustion area to undergo combustion at the temperature of the cylinder wall [51,60]. This results in decreased levels of hydrocarbon (HC) emissions from nanofuel mixes. As can be observed in Figure 10, both the hydrocarbon emissions and the braking power varied during the test.

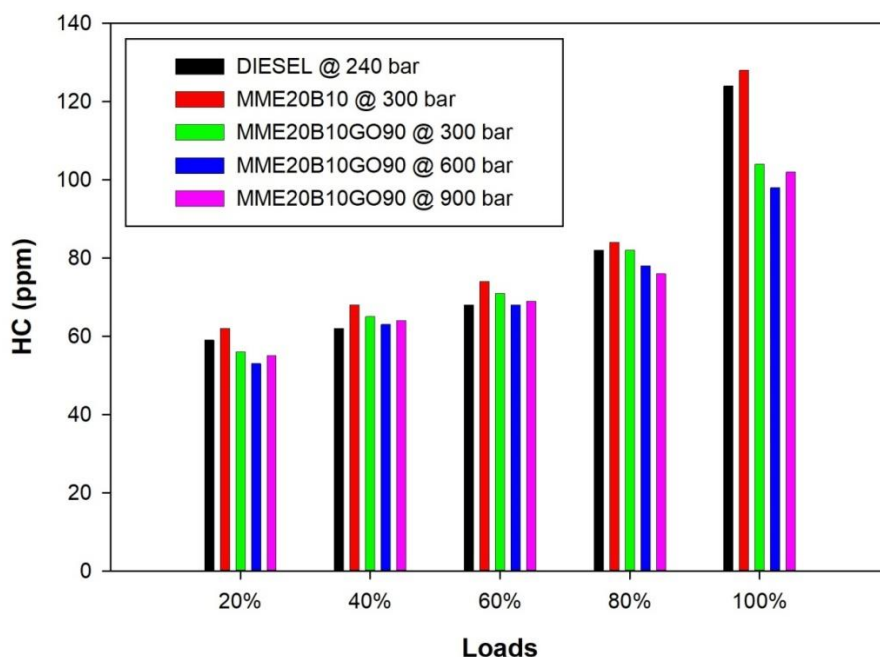


Fig 10: Emission of Hydrocarbons

When compared with Mahua bio diesel, 10% butanol as and GO NP dosages, the Mahua methyl ester (MME20) displayed a significant reduction in the amount of hydrocarbon emissions produced. The lowest HC emissions were found in MME20B10GO90. At maximum speed, the HC emissions from a fuel mix that included 10% butanol and 90 ppm GO NPs were 0.0048 g/kWh. This was lower than the HC emissions from plain diesel by 0.00025 g/kWh and lower than MME20 by 0.2842 g/kWh. The amount of HC emissions decreased by 44.72% as compared with diesel and MME20. The enhanced catalytic activity on the surface of the combustion chamber causes the asymmetric particles of fuel and air to burn more quickly.

11.3 The Impact of Fuel Additives on CO₂ Emissions

In comparison to MME20B10GO90, the graphene oxide nanoparticles included in Mahua biodiesel result in lower CO₂ emissions. At 80% and 100% load, unburned HC increased, increasing CO₂ emissions. Burning hydrocarbons produces CO₂ and water vapour. Figure 11 illustrates both the carbon dioxide emissions and the braking force generated by the test mixture of fuel

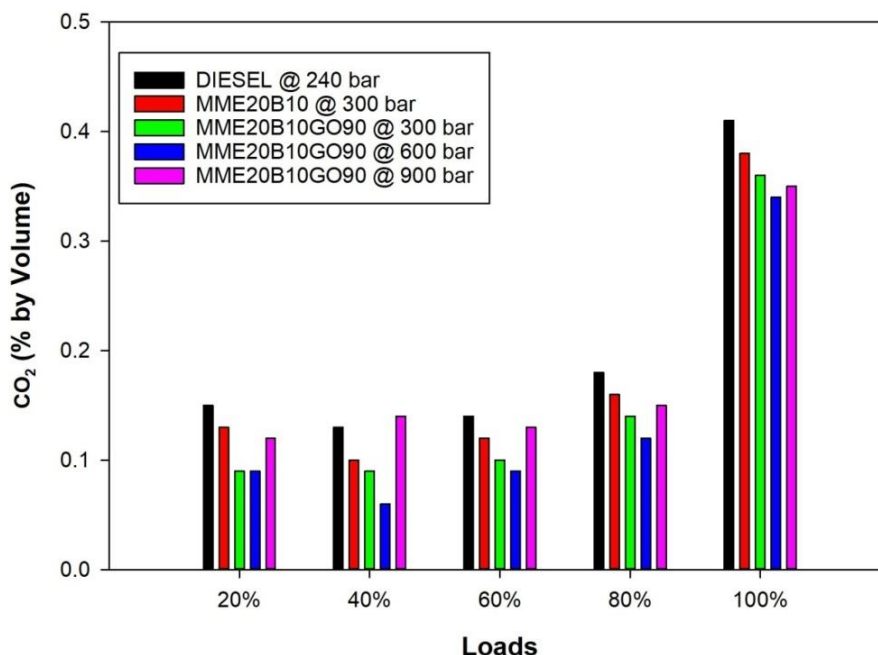


Fig. 11. Emission of Carbon dioxide

Via accumulation 10% n-butanol to the fuel mixture, it is possible to achieve enhanced combustion at temperatures that are both lower in the engine and lower in the combustion chamber. This is made possible by the accumulation of the n-butanol. If the CO₂ emissions produced by the MME20B10GO90 fuel mix are comparable to those produced by diesel fuel at larger loads and burning rates that generate more CO₂, then this shows indicate the fuel is being burnt entirely owing to better oxidation. When compared to MME20, the CO₂ emissions from running at full capacity using nanofuel blends NSME25B10GO90 were much lower. The insufficient combustion of Mahua biodiesel (MME20) was the source of the greatest amount of carbon dioxide that was created.

11.4 The impact of fuel additives and Nitrogen oxide (NO_x) emissions

The combustion chamber's temperature and the amount of O₂ present in it are the two factors that have the greatest impact on the amount of nitrogen oxides produced. The changes that took place in terms of braking power and nitrogen oxide emissions may be seen in Figure 12. These changes took place during the course of the testing. The outcomes of the research indicate that the levels of NO_x emissions generated by MME20 and MME25B10 (GO-90 ppm) are noticeably greater than those produced by diesel.

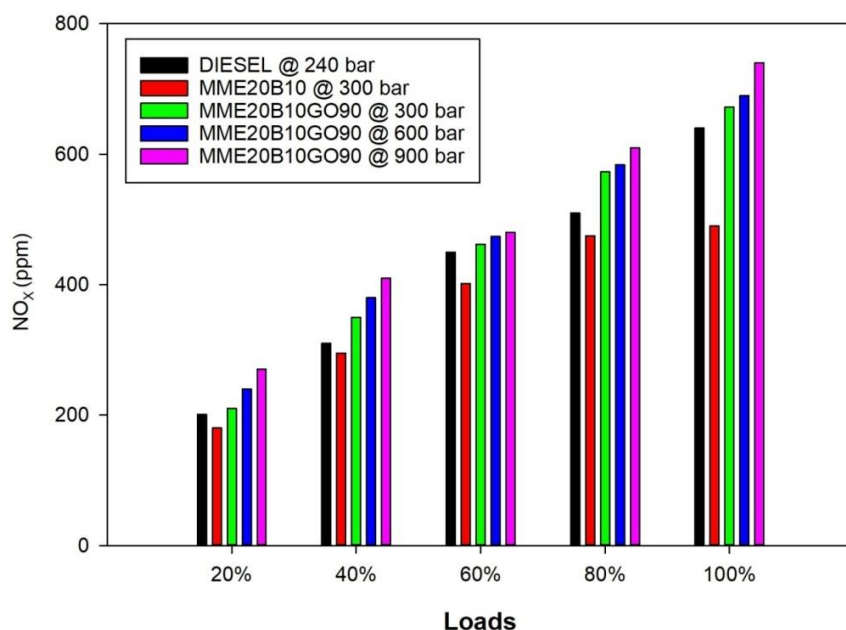


Fig 12: Emission of Nitrous Oxides.

The presence of the oxygen molecules in excessive amounts, the presence of a stabilising agent (Ten % butanol), besides the varying dosages of GO NPs, which give even supplementary O₂ atoms, all contribute to the possibility of high NO_x emissions. All of these factors contribute to the possibility of high NO_x emissions. It's possible that each of these things has a role in the circumstance. A development in peak pressure in the cylinder is another likely cause for increased NO_x emissions, which may also be ascribed to this event in its own right. These high NO_x emissions can be attributed to this occurrence in their own right. When contrasted with diesel's 800 ppm and MME20's 815 ppm, respectively, the nanofuel mix MME20B10GO(90) produces the highest level of NO_x emissions, at 785 parts per million (ppm). This is due to the fact that it includes a high ratio of oxygen-donating GO NPs, in addition to butanol, which is the reason why it has this property.

11.5 The Impact of Smoke-Producing Fuel Additives Graphene oxide nanoparticles activate air and fuel molecules with 180 m²/g asymmetric surface area [3]. Figure 13 shows how MME20B10GO90 Nanofuel blends affect smoke and stopping power. smoke and stopping power.

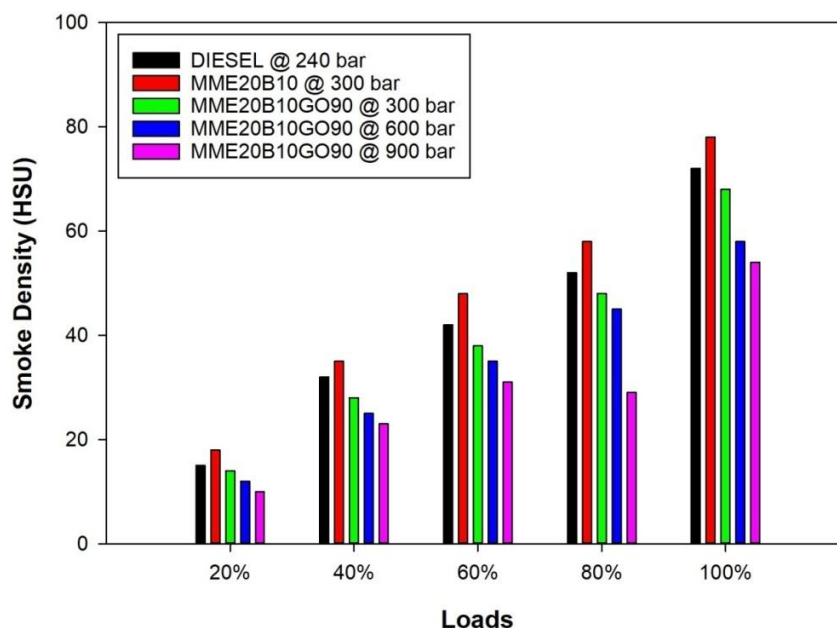


Fig. 13. Smoke Density

Graphene oxide NPs, have a greater thermal conductivity than other nanoparticles, which enables them to transmit appropriate heat to the individual molecule of the byproduct of combustion deposited on the additive surface. The thermal conductivity of graphene oxide nanoparticles (NPs) is 5000 W/mK. Improved atomization, the combustion process, and smoke are all results of butanol's higher oxygen content, reduced viscosity, and lower boiling point. At maximum loads, there is a greater volume of smoke that enters the combustion chamber. The smoke emissions produced by MME20B10GO90 were comparable to those produced by ordinary diesel fuel (72.85 HSU) and MME20 (70.55 HSU). Because of their shorter ID time, nanofuel mixes expedited premixed combustion, which in turn reduced smoke emissions.

Conclusions

The experimentation and research conducted on the CRDI engine with a toroid-shaped combustion chamber and a fuel injector with three holes. In order to lessen the viscosity of biodiesel and the graphene oxide nanoparticle and raise their cetane numbers, a 10% oxygenated addition called N-butanol was added to both of these substances. Additionally, it acted as a catalyst while simultaneously amplifying the phenomena of microexplosions. This section provides a condensed overview of the different effects that Mahua biodiesel (MME20) has on CRDI engines. In order to make this biodiesel, fuel diesel, n-butanol, and asymmetric graphene oxide nanoparticles are mixed together.

Specifically, the BTE of MME20 (an n-butanol and graphene oxide nanoparticles emulsion fuel) is compared to that of MME20B10. was much higher. MME20B10GO90 has a BTE equivalent to diesel fuel. The BTE content of MME20B10GO90 fuel is 19.47% greater than that of MME20 fuel. All nanofuel mixes are catalysed by GO NPs, which results in an improvement in BTE.

Full fuel combustion and a higher air-to-fuel mixing ratio both contributed to a drop in BSFC values across the board for all n-butanol nanofuel mixes. Both the temperature within the cylinder and the amount of oxygen available rose.

Both the pace at which heat was released and the pressure within the cylinder were greatly boosted as a result of the toroidal combustion chamber's greater air-to-fuel mixing. It was possible for this to occur as a result of improvements made to the swirling motion as well as the use of a 3-hole fuel injector that operated at a pressure of 900 bar. In contrast, the MME25, n-butanol, and GO NPs fuel combination generated higher levels of NO_x emissions, whilst the MME20 and diesel-powered vehicles produced lower levels of NO_x emissions. These differences may be attributed to the types of fuels that were used. owing to the high temperatures inside the combustion chamber, an overabundance of oxygen molecules was also a contributing factor in the increased quantities of NO_x emissions that were produced. In the meanwhile, among all of the cars that were put through the test, the MME20B10GO90 had the highest levels of NO_x emissions.

Because of the incorporation of GO NPs into mahua methyl ester, the emissions of smoke, carbon dioxide (CO₂), and hydrocarbons (HC) were all cut down significantly. At maximum load, the MME20B10GO90 fuel blend was able to reduce smoke emissions by 29.85 percent, nitrogen oxides by 42.83 percent, and CO emissions by 42.83 percent, respectively, as compared to the MME20B10 fuel mix.

It has been determined, on the basis of the results of the studies, that Mahua biodiesel should be used. be augmented with 90–120 ppm graphene oxide nanoparticle and 10% n-butanol blend nearly diesel properties. The functionality of the CRDI engine is enhanced as a result. Each possessing an orifice diameter of 0.1 millimetres is the toroidal chamber enabling combustion and the three-hole fuel injector nozzle. millimetres, work together to produce a very high-pressure fuel vapour that burns fuel more rapidly. These two factors make it possible for this to happen.

Nomenclature

NPs	Nanoparticles
CRDI	Common rail direct injection
SCR	Selective catalytic reaction
DEF	Diesel exhaust fluid
GO	Graphene oxide
SDBS	Sodium dodecyl benzene sulphonate
A: F	Air-to-fuel ratio
nm	Nanometer
HRR	Heat release rate
BTE	Brake thermal efficiency
ppm	Parts per million
HC	Hydrocarbon
CO ₂	Carbon dioxide

CO	Carbon monoxide
NOX	Oxides of nitrogen
PM	Particulate matter
BSFC	Brake-specific fuel consumption

References

1. Mohibbe Azam, Amtul, Nahar N.M; "Prospects and potential of fatty acid methyl esters of some non-traditional seed oils for use as biodiesel in India", Journal of biomass and bioenergy, vol 29, pp.293-302, 2005
2. Maykut, N. N.; Lewtas, J.; Kim, E.; Larson, T. V. Source Apportionment of PM_{2.5} at an Urban IMPROVE Site in Seattle, Washington. Environ. Sci. Technol. 2003, 37 (22), 5135–5142.
3. Bosch, R. Bosch Automotive Handbook; Bentley Publishers: Cambridge, MA, 1986
4. Heywood, J. B. Internal Combustion Engine Fundamentals. McGraw Hill: 2001.
5. Choi, B. C. Technologies for Emission After-Treatment. Baro Press 2001, 49–52
6. Ferreira Squaiella, L. L.; Martins, C. A.; Lacava, P. T. Strategies for emission control in diesel engine to meet Euro VI. Fuel 2013, 104, 183–193.
7. Martyr, A. J.; Plint, M. A. Engine Testing: The Design, Building, Modification and Use of Powertrain Test Facilities; Elsevier: New York, 2012.
8. Dodd AE, Holubecki Z. The measurement of diesel exhaust smoke MIRA, Report 1965/10; 1965.
9. Badami, M.; Mallamo, F.; Millo, F.; Rossi, E. Influence of Multiple Injection Strategies on Emissions, Combustion Noise and BSFC of a DI Common Rail Diesel Engine; SAE Technical Paper; SAE International: Warrendale, PA, USA, 2002.
10. Rakopoulos, C.; Dimaratos, A.; Giakoumis, E.; Rakopoulos, D. Study of turbocharged diesel engine operation, pollutant emissions and combustion noise radiation during starting with bio-diesel or nbutanol diesel fuel blends. Appl. Energy 2011, 88 (11), 3905–3916.
11. Luque, R.; Lovett, J. C.; Datta, B.; Clancy, J.; Campelo, J. M.; Romero, A. A. Biodiesel as feasible diesel fuel replacement: a multidisciplinary overview. Energy Environ. Sci. 2010, 3 (11), 1706– 1721.
12. Daming Huang, Haining Zhou , Lin Lin, "Biodiesel: an Alternative to Conventional Fuel", 2012 International Conference on Future Energy, Environment, and Materials,
13. Augustin, U., and Schwarz, V., "Low-Noise Combustion with Pilot Injection," Truck Technology International, 1991.
14. Schulte, Fl., et. al., "The Influence of Pilot Injection on Combustion in DI Diesel Engines," FEV Technical Papers, 1989.
15. Miyaki, M., Fujisawa, H., Masuda, A., and Yamamoto, Y., "Development of New Electronically Controlled Fuel Injection System ECD-U2 for Diesel Engines," SAE Paper 910252, 1991.
16. Shakal, J. and Martin, J. K., "Effects of Auxiliary Injection on Diesel Engine Combustion," SAE Paper 900398, 1990.
17. Shundoh, S., et al., "NO_x Reduction from Diesel Combustion Using Pilot Injection with High Pressure Fuel Injection," SAE Paper 920461, 1992.

18. D. A. Nehmer and R. D. Reitz, "Measurement of the Effect of Injection Rate and Split Injections on Diesel Engine Soot and NOx Emissions", DOI: <https://doi.org/10.4271/940668>, SAE PAPER 940668, 1994
19. Erhard Sitter, Fuel Injection Apparatus With Plot Injection And Man Injection In Internal Combustion Engines, United States Patent US4520774A
20. Gan, Y.; Qiao, L. Combustion characteristics of fuel droplets with addition of nano and micron-sized aluminum particles. *Combust. Flame* 2011, 158 (2), 354–368.
21. Chehroudi, B. Nanotechnology and Applied Combustion: Use of Nanostructured Materials for Light-Activated Distributed Ignition of Fuels with Propulsion Applications. *Recent Patents on Space Technology* 2011, 1 (2), 107–122.
22. Mehta, R. N.; Chakraborty, M.; Parikh, P. A. Nanofuels: Combustion, engine performance and emissions. *Fuel* 2014, 120 (0), 91–97.
23. Sudheer nandi, " Performance of CI Engine by using biodiesel-Mahua oil ", *American Journal of Engineering Research*, vol 02, issue 10, pp. 22-47
24. Pope, C. A., Burnett, R. T.; Thun, M. J.; Calle, E. E.; Krewski, D.; Ito, K.; Thurston, G. D. Lung cancer, cardiopulmonary mortality, and long-term exposure to fine particulate air pollution. *Jama* 2002, 287 (9), 1132–1141.
25. Sharifi, S.; Behzadi, S.; Laurent, S.; Laird Forrest, M.; Stroeve, P.; Mahmoudi, M. Toxicity of nanomaterials. *Chem. Soc. Rev.* 2012, 41 (6), 2323–2343.
26. Kim, F.; Luo, J.; Cruz-Silva, R.; Cote, L. J.; Sohn, K.; Huang, J. Self-Propagating Domino-like Reactions in Oxidized Graphite. *Adv. Funct. Mater.* 2010, 20 (17), 2867–2873.
27. Li, J.-L.; Kudin, K. N.; McAllister, M. J.; Prud'homme, R. K.; Aksay, I. A.; Car, R. Oxygen-Driven Unzipping of Graphitic Materials. *Phys. Rev. Lett.* 2006, 96 (17), 176101.
28. Zhu, Y.; Murali, S.; Cai, W.; Li, X.; Suk, J. W.; Potts, J. R.; Ruoff, R. S. Graphene and graphene oxide: synthesis, properties, and applications. *Adv. Mater.* 2010, 22 (35), 3906–3924.
29. Ahmed I. El-Seesy, Hamdy Hassan , S. Ookawara, "Effects of graphene nanoplatelet addition to jatropha Biodiesel-Diesel mixture on the performance and emission characteristics of a diesel engine", <https://doi.org/10.1016/j.energy.2018.01.108>, Volume 147, 15, Pages 1129-1152, 2018
30. A.I. EL-Seesy, H. Hassan, S. Ookawara, Performance, combustion, and emission characteristics of a diesel engine fueled with Jatropha methyl ester and graphene oxide additives, *Energy Convers. Manag.* 166 (2018) 674–686, <https://doi.org/10.1016/j.enconman.2018.04.049>.
31. Jong Boon Ooi , Harun Mohamed Ismail , Boon Thong Tan a , Xin Wang "Effects of Graphite Oxide and Single-Walled Carbon Nanotubes as 2 Diesel Additives on the Performance, Combustion, and Emission 3 Characteristics of a Light-Duty Diesel Engine", *Renewable Energy*, <https://doi.org/10.1016/j.energy.2018.07.062>, Volume 161, 15, Pages 70-80, October 2018
32. S.S. Hoseini, G. Najafi, B. Ghobadian, R. Mamat, M.T. Ebadi, T. Yusaf "Novel environmentally friendly fuel: The effects of nanographene oxide additives on the performance and emission characteristics of diesel engines fuelled with Ailanthus altissima biodiesel", *Renewable Energy*, <https://doi.org/10.1016/j.renene.2018.02.104>, Volume 125, , Pages 283-294, 2018

33. Ahmed I. EL-Seesya,b, HamdyHassana,c, “Investigation of the Effect of Adding Graphene Oxide, Graphene 2 Nanoplatelet, and Multiwalled Carbon Nanotube Additives with n3 Butanol-Jatropha Methyl Ester on a diesel engine performance”, *Renewable Energy*, DOI:10.1016/j.renene.2018.08.026, 2018
34. Luis Tipanluisaa,d , Natalia Fonseca , Jesús Casanova , Jos´e-María Lopez, “Effect of n-butanol/diesel blends on performance and emissions of a heavy-duty diesel engine tested under the World Harmonised Steady-State cycle” , *Fuel*, <https://doi.org/10.1016/j.fuel.2021.121204>Volume 302, 15, 121204, October 2021
35. K. Siva Prasad, S. Srinivasa Rao & V.R.K. Raju “Performance and emission characteristics of a DIC engine operated with n-butanol/diesel blends” , *Energy Sources, Part A: Recovery, Utilization, And Environmental Effects* <https://doi.org/10.1080/15567036.2019.1685611>, 2019
36. Ashish Nayyar , Dilip Sharma , Shyam Lal Soni , Alok Mathur · Experimental investigation of performance and emissions of a VCR diesel engine fuelled with n-butanol diesel blends under varying engine parameters. *Environ Sci Pollut Res* 24:20315–29. doi:10.1007/s11356-017-9599-8.
37. Nadir Yilmaz , Francisco M. Vigil, Kyle Benalil, Stephen M. Davis, Antonio Calva “Effect of biodiesel–butanol fuel blends on emissions and performance characteristics of a diesel engine”, *Feul*, <https://doi.org/10.1016/j.fuel.2014.06.022>, Volume 135, 1 Pages 46-50, November 2014
38. S.Imtenan, H.H.MasjukiM.VarmanI.M.Rizwanul FattahH.SajjadM.I.Arbab “Effect of n-butanol and diethyl ether as oxygenated additives on combustion–emission-performance characteristics of a multiple cylinder diesel engine fuelled with diesel–jatropha biodiesel blend”, *Energy Conversion and Management*, <https://doi.org/10.1016/j.enconman.2015.01.047>, Volume 94, , Pages 84-94, April 2015
39. Dimitrios C. Rakopoulos , Constantine D. Rakopoulos , Evangelos G. Giakoumis , Roussos G. Papagiannakis , Dimitrios C. Kyritsis c, “Influence of properties of various common bio-fuels on the combustion and emission characteristics of high-speed DI (direct injection) diesel engine: Vegetable oil, bio-diesel, ethanol, n-butanol, diethyl ether”, *Energy*, DOI:10.1016/j.energy.2014.06.032
40. Atmanli A, Yuksel B, Ileri E ,”Experimental investigation of the effect of diesel–cotton oil–n-butanol ternary blends on phase stability, engine performance and exhaust emission parameters in a diesel engine”., *Fuel*, <https://doi.org/10.1016/j.fuel.2013.03.012> 109:503–511, Volume 109, July 2013, Pages 503-511
41. Atmanli A, Ileri E, Yuksel B “ Experimental investigation of engine performance and exhaust emissions of a diesel engine fueled with diesel–n-butanol–vegetable oil blends”. *Energy Conversion and Management*, <https://doi.org/10.1016/j.enconman.2014.02.049>, Volume 81, May 2014, Pages 312-321
42. Atmanli A, Ileri E, Yuksel B, Yilmaz N,Extensive analyses of diesel–vegetable oil–n-butanol ternary blends in a diesel engine. *Applied Energy*, <https://doi.org/10.1016/j.apenergy.2015.01.071> , Volume 145, 1 May 2015, Pages 155-162
43. Manzoore Elahi. M. Soudagara,, Nik-Nazri Nik-Ghazalia,, M.A. Kalama , Irfan Anjum Badruddinb , N.R. Banapurmathc , T.M. YunusKhanb , M. Nasir Bashira , Naveed Akrama , RijavanFaraded , Asif Afzale “The effects of graphene oxide nanoparticle additive stably

- dispersed in dairy scum oil biodiesel-diesel fuel blend on CI engine: performance, emission and combustion characteristics”, *Fuel*, <https://doi.org/10.1016/j.fuel.2019.116015> Volume 257, 1 December 2019, 116015
44. S.S. Hoseini , G. Najafi a, B. Ghobadian , M.T. Ebadi , R. Mamat , T. Yusaf , “Biodiesels from three feedstock: The effect of graphene oxide (GO) nanoparticles diesel engine parameters fuelled with biodiesel”, *Renewable Energy*, <https://doi.org/10.1016/j.renene.2019.06.020>, Volume 145, January 2020, Pages 190-201
 45. S.S. Hoseini , G. Najafi a, B. Ghobadian a , M.T. Ebadi a , R. Mamat b , T. Yusaf, “Performance and emission characteristics of a CI engine using graphene oxide (GO) nanoparticles additives in biodiesel-diesel blends”, *Renewable Energy* <https://doi.org/10.1016/j.renene.2019.06.006>, Volume 145, January 2020, Pages 458-465
 46. Sabourin, J. L.; Dabbs, D. M.; Yetter, R. A.; Dryer, F. L.; Aksay, I. A. Functionalized graphene sheet colloids for enhanced fuel/ propellant combustion. *ACS Nano* 2009, 3 (12), 3945–3954.
 47. D.K.Bora, M.pally, V.Sanduja, “Performance evaluation and emission characteristics of a diesel engine using Mahua oil Methyl ester (MOME).SAE:10.4271/2004-28-0034
 48. Freedman B, Pryde EH, Mounts TL. Variables affecting the yields of fatty esters from transesterified vegetable oils. *Journal of American Oil Chemists Society* 1984;61(10): 1638–43
 49. Fangrui MA, Hanna MA. Biodiesel production a review. *Bioresource Technology* 1999;70(1):1–15.
 50. E. Griffin Shay ” Diesel Fuel From Vegetable Oils: Status And Opportunities” National Academy of Sciences, 2101 Constitution Avenue, Washington, DC 20418, U.S.A., [https://doi.org/10.1016/0961-9534\(93\)90080-N](https://doi.org/10.1016/0961-9534(93)90080-N), Vol. 4, No. 4, pp. 227242, 1993
 51. Vijayakumar Chandrasekaran , Murugesan Arthanarisamy b , PanneerselvamNachiappan c , Subramaniam Dhanakotti b , Bharathiraja Moorthy, “The role of nano additives for biodiesel and diesel blended transportation fuels” *Transportation Research Part D: Transport and Environment*, <http://dx.doi.org/10.1016/j.trd.2016.03.015>, Volume 46, , Pages 145-156, July 2016
 52. Jong Boon Ooi, Harun Mohamed Ismail, Varghese Swamy, Xin Wang, Akshaya Kumar Swain, and Jeevan Raj Rajanren, Graphite Oxide Nanoparticle as a Diesel Fuel Additive for Cleaner Emissions and Lower Fuel Consumption. <https://doi.org/10.1021/acs.energyfuels.5b02162>, *Energy Fuels* 2016, 5, 02162
 53. Hurmathulla Khan , Manzoore Elahi M. Soudagar , Rajagopal Harish Kumar , Mohammad Reza Safaei , Muhammad Farooq , AbdulqhadarKhidmatgar , Nagaraj R Banapurmath , Rizwan A. Farade , Muhammad Mujtaba Abbas , Asif Afzal , Waqar Ahmed , MarjanGoodarzi and Syed NoemanTaqui , “Effect of Nano-Graphene Oxide and n-Butanol Fuel Additives Blended with Diesel—Nigella sativa Biodiesel Fuel Emulsion on Diesel Engine Characteristics”,*Symmetry* , DOI:10.1016/j.fuproc.2020.106406 2020
 54. Guoan Li Quan Zhang “Sodium dodecyl benzene sulfonate aqueous solution and preparation method thereof and application”, CN101632353B
 55. B M Paramashivaiah1 and C R Rajashekhar “Studies on effect of various surfactants on stable dispersion of graphene nano particles in simarouba biodiesel”, *IOP Conf. Series: Materials Science and Engineering* 149 (2016) 012083 doi:10.1088/1757-899X/149/1/012083

56. Wickham, D. T.; Cook, R. L.; Engel, J.; Jones, M.; Nabity, J. Soluble Nanocatalysts for High Performance Fuels. Presented at the 19th ONR Propulsion Meeting, Los Angeles, CA, December 20, 2006.
57. Wickham, D. T.; Cook, R. L.; De Voss, S.; Engel, J. R.; Nabity, J. Soluble Nanocatalysts for High Performance Fuels. *J. Russ. Laser Res.* 2006, 27, 552–561.
58. Linda Vaisman, H. Daniel Wagner, Gad Marom, The role of surfactants in dispersion of carbon nanotubes, *Advances in Colloid and Interface Science* 128–130 (2006) 37–46.
59. Richa Rastogi, Rahul Kaushal, S.K. Tripathi, Amit L. Sharma, Inderpreet Kaur, Lalit M. Bharadwaj, Comparative study of carbon nanotube dispersion using surfactants, *Journal of Colloid and Interface Science* 328 (2008) 421–428.